PERGAMON

Computerized Medical Imaging and Graphics 22 (1998) 399–408

Computerized Medical Imaging and Graphics

A pyramidal approach for automatic segmentation of multiple sclerosis lesions in brain MRI

C. Pachai[a,*], Y.M. Zhu[a], J. Grimaud[b], M. Hermier[c], A. Dromigny-Badin[a], A. Boudraa[a], G. Gimenez[a], C. Confavreux[b], J.C. Froment[c]

[a]*CREATIS, CNRS Research Unit UMR 5515, INSA 502, 69621 Villeurbanne, France*
[b]*Department of Neurology, Hôpital Neurologique et Neurochirurgical, 69394 Lyon, France*
[c]*Department of Radiology-MRI, Hôpital Neurologique et Neurochirurgical, 69394 Lyon, France*

Received 27 March 1998; received in revised form 17 September 1998

Abstract

Quantitative assessment of Magnetic Resonance Imaging (MRI) lesion load of patients with multiple sclerosis (MS) is the most objective approach for a better understanding of the history of the pathology, either natural or modified by therapies. To achieve an accurate and reproducible quantification of MS lesions in conventional brain MRI, an automatic segmentation algorithm based on a multiresolution approach using pyramidal data structures is proposed. The systematic pyramidal decomposition in the frequency domain provides a robust and flexible low level tool for MR image analysis. Context-dependent rules regarding MRI findings in MS are used as high level considerations for automatic lesion detection.

Keywords: Segmentation; Image analysis; Pyramid; Multiresolution; MRI; Multiple sclerosis

1. Introduction

Multiple sclerosis (MS) is the most common disabling neurological disease among young adults in North America and northern Europe. Assessing the clinical outcome of patients with MS is usually achieved through subjective considerations such as the use of disability status scales (e.g. Extended Disability Status Scale: EDSS). However, this does not provide a good understanding of the long and complex history of the pathology either natural or modified by therapies. Magnetic Resonance Imaging (MRI) has become the most sensitive paraclinical test to assess the morphology and topography of MS lesions in the human brain. Since the late 1980s, the clinical evaluation of patients with MS has been fundamentally changed by the introduction of MRI techniques, which give an objective signature of the pathology even in its early stages. Although the diagnosis is principally based on a neurological examination and the history of characteristic symptoms, brain MRI represents a major confirmatory test for MS (abnormal scans in more than 90% of cases) [1,2]. The MRI description of the topography of MS lesions (dissemination of the disease in space) and the possibility offered by serial MRI to assess disease activity (dissemination of lesions in time) are used for diagnosis purposes [1,3], monitoring disease evolution and treatment trials [4–6]. In this context, quantitative assessment of MRI lesion load is of major interest.

Manual outlining and semi-automated intensity-based techniques are used by some of the current major protocols for MS lesion detection and quantification in MRI. These techniques are heavily time-consuming, with low reproducibility [3]. Faster techniques with higher reproducibility are still needed [5]. Any image processing environment which aims to improve the overall reproducibility must provide automatic tools for tackling the segmentation of MRI data. Any human intervention to initiate semi-automated segmentation algorithms (e.g. setting gray level thresholds or initial seeds within a zone of interest for region growing algorithms) inevitably leads to subjective considerations, which reduce the reproducibility of the quantitative assessment. Many research teams have already proposed automatic algorithms for MS lesions segmentation and quantification [7–12], with solutions to handle partial volume effect and radio frequency inhomogeneity [13–15].

The automatic segmentation of MS lesions in MRI, however, remains a persistent problem. Although the histopathology of MS shows that lesions essentially belong to

* Corresponding author. Tel.: + 33-472-43-87-86; fax: + 33-472-43-85-26; e-mail: pachai@creatis.insa-lyon.fr.

0895-6111/98/$ - see front matter
PII: S0895-6111(98)00049-4

white matter with a rate of 95% and the remaining in gray matter [1], with a typical periventricular location, it is not possible to use any *topographical* hypothesis to make their recognition easier. MS lesions may appear at any location within white or gray matter. The *morphology* of MS lesions also has variable characteristics. Lesions may be from a few millimeters to several centimeters in length, focal or confluent and their shapes can be ovoid or long. Vague areas with less important increased signal often surround them [1,16]. Hence, their contours may be more or less easy to detect. In such a context, the segmentation algorithm must be sufficiently sensitive to detect any region of increased signal, regardless of its position and the local value of image intensity. A global thresholding scheme cannot be a consistent approach for lesion detection. The signal intensity of two distant lesions may not have similar means and variances. Their contrast with the surrounding white matter may be completely different. It is then impossible to do any calibration of the signal intensity distribution with respect to white matter to work out an intensity-based signature of MS lesions. This is due to the MRI inherent radio-frequency inhomogeneity and to the fact that two distant lesions may be at two different stages of their natural evolution with, probably, different signal intensity. This is one of the major problems of intensity-based statistical classification techniques where multispectral MRI data are used [11,13].

The aim of this paper is to describe how a low-level segmentation tool may decrease the overall complexity of MR image analysis for lesion detection. The main contribution of such a low-level assessment is that it provides an automatic way of extracting special features from MR images. It is then possible to focus on smaller regions of interest for further segmentation and to carry out shape recognition approaches for high level considerations. To deal with the random characteristics of MS lesions, as far as morphology, topography and signal-intensity are concerned, we perform a sensitive and local detection of hyperintense features using a multiresolution approach on proton density (PD) and T2-weighted spin echo sequences (repetition time: TR = 2500 ms; echo time: TE_{PD} = 20 ms, TE_{T2} = 90 ms; axial slices of 5 mm thickness; image size 256 × 256 pixels), acquired on a Siemens 1.5 Tesla Magnetom Vision. The technique may be considered as a flexible low-level segmentation tool to be used with brain MR images. By flexibility, we mean taking into account high level considerations such as tracking 'hyperintense' or 'hypointense' features within a given image, and selecting convenient degrees of resolution to assign some sort of priority with respect to the size of the objects which must be detected. The algorithm uses pyramidal data structures to provide a multiresolution representation of a given MR image. By means of successive Gaussian filtering operations, we obtain different low-pass versions of the initial image (Gaussian pyramid), while subtractions between the initial image and different levels of the Gaussian pyramid give a multiresolution high-pass representation of that image (Laplacian pyramid). As far as the signal of MS lesions in PD and T2-weighted images is more or less hyperintense, the multiresolution algorithm must detect local variations of signal intensity whatever the importance of the corresponding gradients. A Laplacian pyramid typically enhances all hyperintense features of a given image and makes their segmentation easier. A given MS lesion is first enhanced at different levels of the pyramid regarding its signal intensity and morphology. An automatic and local thresholding algorithm then achieves the actual segmentation of the enhanced pixels.

The paper is organized as follows. Section 2 gives a brief recall of multiresolution and pyramidal concepts. In Section 3, we give a thorough description of the pyramidal segmentation algorithm. The overall performance of the proposed technique is discussed in Section 4 in terms of its suitability to solve different problems regarding the automatic segmentation of MS lesions in MRI.

2. Pyramidal models

The human eye looking at a given object while moving away from it, can serve as a model for the idea of decreasing size or diminishing resolution. A multiresolution model is based upon this visual impression. It consists of generating different versions of a given image by decreasing the initial resolution. From a *spatial* point of view, decreasing the initial resolution also means decreasing the initial size. This is achieved by a down-sampling operator which must be associated with an appropriate filtering to avoid aliasing phenomena (down-sampling theorem). From an *informational* point of view, if we bring all the images with different resolutions back to the initial size, by means of appropriate up-sampling operations, we can note a diminution of precision and details, in other words, a simplification of the contents of the initial image. The interesting analogy between the human visual system and multiresolution approaches has been investigated for different purposes such as image segmentation [17,18], image compression [19] and parallel implementation of multiresolution algorithm [20]. In terms of image analysis, low-resolution representations are convenient for global detection and recognition of image features while minute details can only be seen on high-resolution images.

A pyramid associated with an image is a data structure, which contains different versions of that image at different resolutions. The initial image is usually the base of such a pyramid. A pyramidal model is both a model for data representation and a model for data processing [20]. The former concerns the ability of such a model to give more compact representations of a given image and hence, an important contribution to image compression and transmission [19]. The latter essentially addresses the efficacy of its implementation (recursive schemes, parallelism). A generating kernel or weighting mask may be used to obtain the *N*th level of the

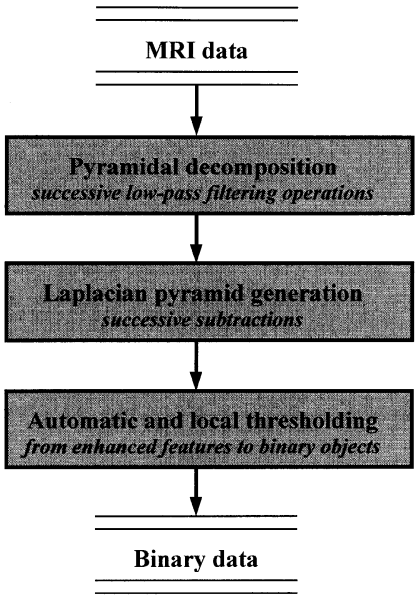

Fig. 1. Pyramidal segmentation.

pyramid from the $N-1$th level. The pyramid construction is completely conditioned by the properties of the generating kernel.

3. Pyramidal segmentation

Fig. 1 illustrates the main steps of the segmentation algorithm, which consists of a pyramidal Gaussian decomposition, Laplacian pyramid generation and automatic thresholding.

3.1. Gaussian pyramid generation

We used the generating kernels proposed by Burt et al. [19], specified to fulfill the following constraints ($k = 5$ is the filter size).

Normalization, in order to conserve the initial image range:

$$\sum_{i=1}^{i=k-1}\sum_{j=0}^{j=k-1} W(i,j) = 1 \tag{1}$$

Symmetry, same contribution of adjacent pixels:

$$W(i,j) = W(k-1-i,j) = W(i,k-1-j) = W(k-1-i,k-1-j) \tag{2}$$

Unimodality, with important weighting coefficients at the center of the mask:

$$0 \le W(i,j) \le W(p,q)$$

$$i \le p \le k/2 \tag{3}$$

$$j \le q \le k/2$$

Equal contribution to the upper kernel, that is to say, all the nodes at a given level must contribute the same total weight ($= 1/4$) to nodes at the next higher level:

$$\sum_{i=0}^{i=1}\sum_{j=0}^{j=1} W(i+2x, j+2y) = 1/4 \tag{4}$$

$$\forall(x,y)\ (W(a,b) = 0 \text{ if } a > k-1 \text{ or } b > k-1)$$

With $W(m,n)$ ($m = 0,1,2$; $n = 0,1,2$) and $\hat{W}$, its one-dimensional version of length 5, these constraints become for a separable filter:

$$\text{Separable}: \quad W(m,n) = \hat{W}(m)\hat{W}(n) \tag{5}$$

$$\text{Normalized}: \quad \sum_{m=-2}^{2} \hat{W}(m) = 1 \tag{6}$$

$$\text{Symmetrical}: \quad \hat{W}(m) = \hat{W}(-m) \quad m = 0,1,2 \tag{7}$$

Equal contribution:

$$\text{If } \hat{W}(0) = a,\ \hat{W}(-1) = \hat{W}(1) = b \text{ and } \hat{W}(-2) = \hat{W}(2) = c \tag{8}$$

Then equal contribution requires that $a + 2c = 2b$.

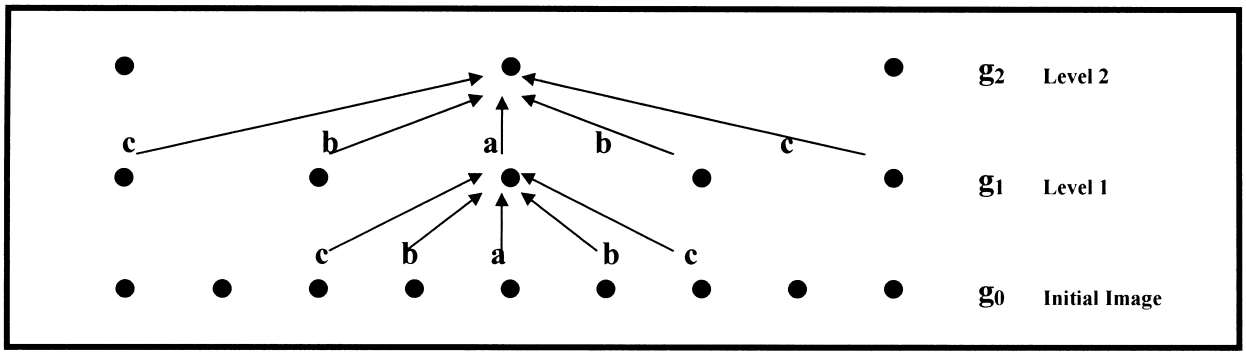

Fig. 2. Gaussian pyramid.

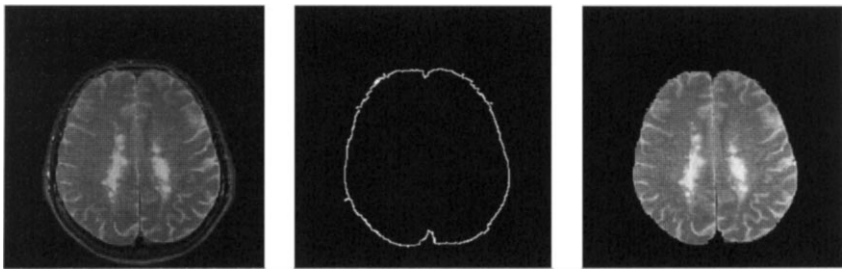

Fig. 3. Internal cavity extraction. Left: original T2-weighted image (256 × 256 pixels). Middle: intracranial cavity contour. Right: region of interest representing the intracranial cavity.

These conditions are fulfilled with

$$\hat{W}(0) = a,\ \hat{W}(-1) = \hat{W}(1) = 1/4,\ \hat{W}(-2) = \hat{W}(2) = 1/4 - a/2 \tag{9}$$

The Gaussian pyramid is then generated by using a so-called *REDUCE* function within the following recurrence:

g_0 : Initial image

$$g_l = REDUCE(g_{l-1}) \tag{10}$$

$$g_l(i,j) = \sum_{m=-2}^{2} \sum_{n=-2}^{2} W(m,n) g_{l-1}(2i+m, 2j+n)$$

The same generating kernel is used at each level of the pyramid (Fig. 2). With $a = 0.4$, the generating kernel has a Gaussian profile [19]. The algorithm reduces the frequency bandwidth from one level to another. The down-sampling factor is 2. The successive Gaussian filtering operations give a set of low-pass filtered versions of the original image.

The detection is carried out only within the intracranial cavity (Fig. 3). Such a region of interest removes features like skull, venous sinus, muscles, fat and eyeballs, making the recognition of MS lesions easier. The intracranial cavity has been extracted using a software developed in our laboratory. Fig. 4 shows the corresponding Gaussian pyramid. With an initial image of size $2^N \times 2^N$, the pyramid may have $N + 1$ different levels of resolution.

We now bring the size of any level of the Gaussian pyramid back to the size of the initial image by means of adequate interpolation and up-sampling operators to obtain the associated expanded Gaussian pyramid (Fig. 5, upper row). This may be achieved recursively by a so-called *EXPAND* function and using the same generating kernel $W(i,j)$.

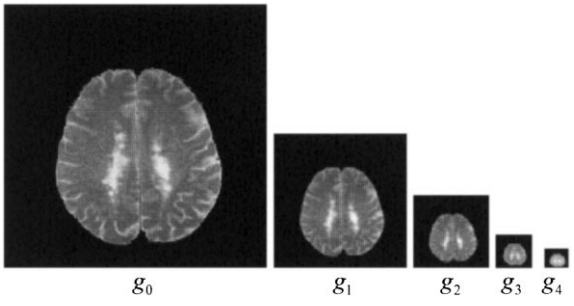

Fig. 4. First five levels of the Gaussian pyramid for the region of interest. The original image, level 0, measures 256 by 256 pixels, and each higher level image is half the dimensions of its predecessor.

g_l : A level of the Gaussian pyramid

$g_{l,n}$: g_l, after applying *EXPAND* n times

$$g_{l,n} = EXPAND(g_{l,n-1}) \tag{11}$$

$$g_{l,n}(i,j) = 4 \sum_{m=-2}^{2} \sum_{n=-2}^{2} W(m,n) g_{l,n-1}\left(\frac{i-m}{2}, \frac{j-n}{2}\right)$$

where $\frac{i-m}{2}, \frac{j-n}{2}$ are integers.

3.2. Laplacian pyramid generation

To perform a sensitive detection of hyperintense features on PD and T2-weighted MRI data, we consider the original image kept in the base of the Gaussian pyramid as a 'reference'. To track its hyperintense features at different resolutions (from fine to coarse), we may successively subtract each level of the expanded Gaussian pyramid from it to obtain an error or Laplacian pyramid. Within this multiresolution scheme, edges correspond to zero-crossings of the error signal. We keep at each resolution the complete hyperintense region corresponding to either the positive or the negative part of the error signal. This 'zero clipping' dramatically simplifies the segmentation of hyperintense features by removing non-relevant parts of the Laplacian pyramid (pixels reset at the background value). The Laplacian pyramid shown in Fig. 5 (lower row) represents the squared positive error, linearly scaled between the minimum (zero) and the maximum values. Burt et al. [19] subtracted two successive levels of their Gaussian pyramid to reduce the entropy of the initial image and for the purposes of data compression and transmission. The use of the initial image as a reference gave us the best sensitivity to track hyperintense features in both PD and T2-weighted MRI data. These are enhanced with respect to their size: fine details may be seen at the bottom of the pyramid while progressively coarser features should be tracked at the top of the pyramid. The

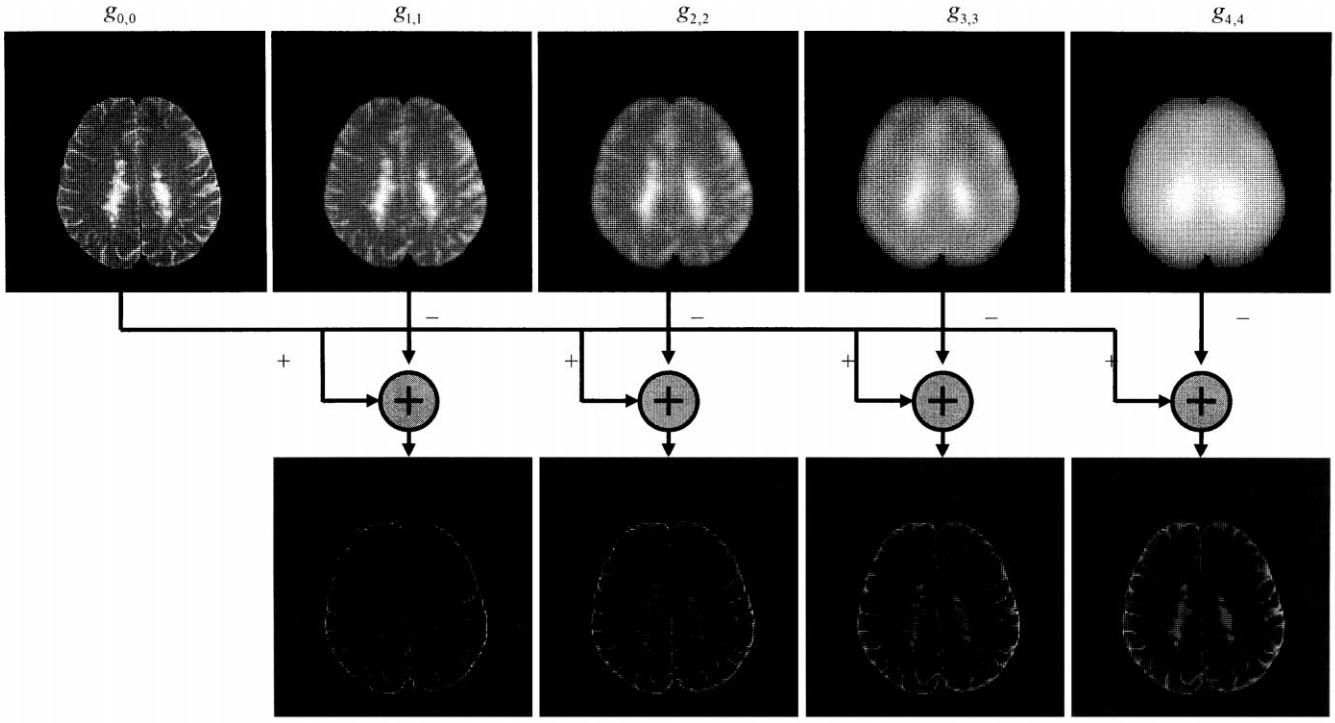

Fig. 5. First five levels of the expanded Gaussian pyramid (upper row) and first four levels of the Laplacian pyramid. Unlike Burt's approach [19], each level of the Laplacian pyramid is the difference between the initial image and the corresponding level of the expanded Gaussian pyramid. Only the positive part of the error signal is kept to enhance hyperintense features.

visual impression confirms both the idea of decreasing the amount of details (expanded Gaussian pyramid) and the idea of selective image feature enhancement with respect to morphology and signal intensity (Laplacian pyramid).

3.3. Automatic local thresholding of the Laplacian pyramid

Enhanced features of the Laplacian pyramid are now much easier to detect than the corresponding hyperintense areas within the original image. We used an automatic and local thresholding algorithm to get binary data from the enhanced pixels of the Laplacian pyramid. For this purpose, we implemented the algorithm proposed by Chow et al. [21], which dynamically determines thresholds according to local characteristics, estimated from the observed intensity histograms of an error image. It assumes that a mixture of two normal intensity distributions characterizes each local region of the image containing a portion of a given boundary. The histogram of such a region will exhibit two peaks and a valley. The thresholding procedure is then as follows:

(a) divide the entire error image into a set of smaller, overlapping regions
(b) compute the histogram for each region
(c) select histograms with large variances
(d) for each selected histogram, estimate the component distributions and coefficient of mixture using a curve fitting algorithm
(e) test the resultant mixtures of estimated distributions for bimodality
(f) for every histogram with appreciable bimodality, calculate the threshold from the estimated distributions by the method of maximum likelihood
(g) interpolate from the thresholds calculated in (f) thresholds for all image points
(h) perform the binary decision for each image point using the threshold obtained in (g).

An input error image of size 256×256 is divided into a 3×3 region of 128×128 pixels with 50% overlap. An intensity histogram is computed over each region. When the region contains a boundary, its corresponding histogram is bimodal. The variance is then computed for each of the nine regions. Larger variances do occur near the boundary. The histogram of a given area is modeled by a normal intensity distribution:

$$f(x) = \sum_{k=1}^{2} p_k \exp\left\{-\frac{(x-\mu_k)^2}{2\sigma_k^2}\right\} \tag{12}$$

where p_1 and p_2 are the theoretical fractions of the given region occupied by the object and the background ($p_1 + p_2 = 1$), μ_1 and μ_2 the means, and σ_1 and σ_2 the variances of the distributions associated with the object and its background. To each of the histograms, $f(x)$ is least-squares fitted by adjusting the five parameters p_1, μ_1, μ_2, σ_1 and σ_2. For the fitting algorithm, we used the

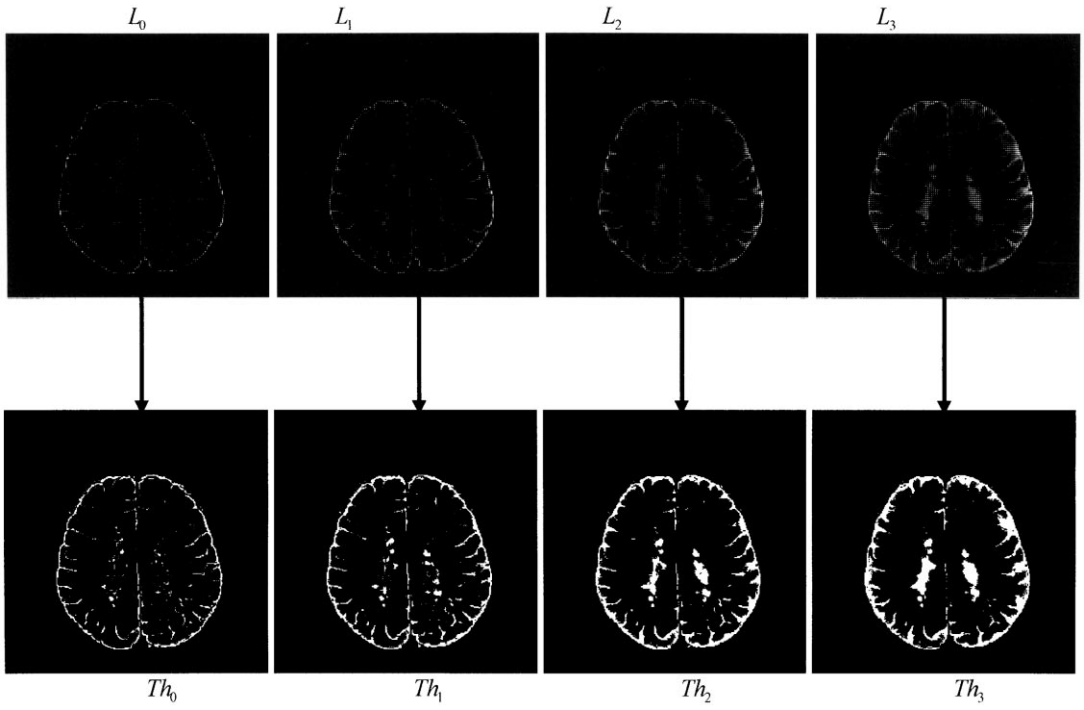

Fig. 6. Automatic thresholding of the Laplacian pyramid.

Levenberg–Marquardt approach, which is explained and implemented in Ref. [22]. This method was chosen because we have to solve the fitting problem when the model depends nonlinearly on the set of several unknown parameters.

When a region contains a distinctive boundary, the resulting histogram shows a bimodal aspect with a deep valley between two peaks. Otherwise, the histogram is monomodal. This bimodality is measured by the valley-to-peak ratio defined by Ref. [6]:

$$\delta = \frac{\min f(x), x \in [\mu_1, \mu_2]}{\min(f(\mu_1), f(\mu_2))} \tag{13}$$

To obtain reliable results, thresholds are computed only from histograms with appreciable bimodality ($\delta \leq 0.8$ in the present study). The threshold computation is performed according to the following quadratic formula derived from the method of maximum likelihood for the value of t which minimizes the probability of misclassification:

$$\left(\frac{1}{\sigma_1^2} - \frac{1}{\sigma_2^2}\right)t^2 + 2\left(\frac{\mu_2}{\sigma_1^2} - \frac{\mu_1}{\sigma_2^2}\right)t + \frac{\mu_1^2}{\sigma_1^2} - \frac{\mu_2^2}{\sigma_2^2} + 2\ln\frac{p_2}{p_1} = 0 \tag{14}$$

At this stage, some regions are not assigned thresholds because of their flat histograms. For these regions, their thresholds are obtained as weighted averages of the computed thresholds of their neighboring regions (a region-wise interpolation). A second interpolation is carried out in a pointwise manner, to ensure continuity in the boundary at the border of two neighboring regions with different thresholds. Within each region, the initially computed threshold is considered valid only at the center point of the region but not necessary all over the entire region. The thresholds for the remaining image points of the region are interpolated from this threshold and those of neighboring regions. An example of the corresponding binary pyramid is shown in Fig. 6 (lower row). Fine details appear in high-resolution images while progressively coarser features may be seen at the top of the pyramid.

3.4. Post-processing

After the automatic thresholding step, we obtain a binary data set representing hyperintense features of the original MR image. To work out the final segmented image and using the list of pixels corresponding to the contour of the intracranial cavity, we automatically remove at each resolution, the binary object that coincides with the external cerebrospinal fluid (CSF). We then perform a logical OR between the first four levels of the binary pyramid (for each pixel). This combination of different resolutions is sufficient to detect even big lesions. After filling holes in binary objects, a two dimensional component labeling algorithm is applied to quantify the binary objects. Those smaller than 3 pixels are removed to follow a usual recommendation of some of MS lesion quantification protocols (e.g. The European Magnetic Resonance Network in Multiple Sclerosis, the MAGNIMS protocols).

On T2-weighted images, CSF which is as hyperintense as

Fig. 7. Automatic results. Left: initial image. Middle: binary objects obtained after a logical OR operation among the first four levels of the binary pyramid. Right: the remaining binary objects after automatic removal of external CSF.

MS lesions is completely detected. At high resolutions, the important discontinuity at the boundaries of the intracranial cavity (masking effect) does not affect the accuracy of the detection of the external CSF (Fig. 7). Small subcortical lesions remain disconnected from the external CSF at high resolutions and are taken into account by the logical OR operation. As the resolution decreases, the binary object representing the external CSF becomes larger and loses its initial morphological accuracy. The post-processing removes contiguous pixels corresponding to the external CSF. Each resolution contributes to the final list of binary objects regardless of where or at which resolution a given feature is enhanced and segmented. This guarantees a systematic and automatic detection of any hyperintense feature without any prior hypothesis regarding its location, its morphology and the corresponding signal gradient.

On PD-weighted images, MS lesions are more hyperintense than CSF. The CSF signal is all the less bright as the Echo Time (TE) is short. Compared with T2-weighted images, CSF/lesions distinction is easier, especially in the periventricular area. Nevertheless, in PD-weighted data, gray matter and MS lesions have similar characteristics in terms of signal intensity and frequency bandwidth. Gray matter hyperintense pixels are hence automatically detected. The signal and the contrast of gray matter on PD-weighted data is much less consistent than those of CSF in T2-weighted data. This lack of consistency generates randomly located false positives.

MS lesions are correctly detected, but false positive pixels representing CSF and gray matter are also in the final list of binary objects respectively on T2 and PD-weighted data. By presenting original data and the binary objects obtained from the segmentation of both PD and T2-weighted data sets to a medical expert, a manual correction is carried out based on removing/keeping decisions and using a computer mouse. Once this is achieved on the entire head, a final quantification is performed to work out the total lesion load corresponding to that study. Fig. 8 shows a manually corrected image.

4. Results and discussion

The algorithms have been implemented using the C language under the UNIX operating system, and LIBIDO, the image processing-oriented library developed in our laboratory. This library provides useful functions written in C. An XMotif/XWindows based graphical user interface has been designed for selecting MR images, executing the algorithms described above and visualizing intermediary pyramids. This interface also provides interactive possibilities to remove false positives for the evaluation of the overall performance by medical experts. The automatic segmentation and quantification of one axial PD or T2-weighted image takes less than 10 s on a Digital DEC 500/400 MHz (256 MB RAM). A complete conventional study (cf. Section 1) with 5 mm thickness images (typically 23 PD and 23 T2-weighted slices) is automatically

```
Number_Of_Objects =10 (Area > 3 pixels)
  Area_In_Pixel(1)    = 4    pixels
  Area_In_Pixel(2)    = 5    pixels
  Area_In_Pixel(3)    = 55   pixels
  Area_In_Pixel(4)    = 22   pixels
  Area_In_Pixel(5)    = 41   pixels
  Area_In_Pixel(6)    = 378  pixels
  Area_In_Pixel(7)    = 347  pixels
  Area_In_Pixel(8)    = 9    pixels
  Area_In_Pixel(9)    = 23   pixels
  Area_In_Pixel(10)   = 10   pixels
-----------------------------------------------
Total_Area_In_Pixel  = 894 pixels
```

Fig. 8. Final result after manual correction (on an acceptance/rejection basis) and lesion load quantification.

processed in less than 12 min (assuming intra-cranial cavity already segmented and corresponding masks available). The average time required to perform manual correction on all slices of a study is 15 min (10 studies). The automatic MRI data processing and the manual correction steps are also much less time consuming. The effect of the medical expert's interventions (either acceptance or rejection) on the reproducibility is much less important than a completely manual or even a semi-automated intensity-based technique. The overall inter- and intra-observer reproducibility are improved. The systematic detection of hyperintense features produces a very low false negative rate. MS lesions are detected with a good morphological accuracy.

On T2-weighted images, external and ventricular CSF are as hyperintense as MS lesions. An accurate segmentation of all hyperintense features is achieved regardless of their shapes and the importance of the corresponding signal intensity gradient. This step is an important pre-segmentation, which dramatically decreases the region of interest for MS lesion detection. Nevertheless, the ventricular CSF is completely segmented and the corresponding binary objects may be contiguous with periventricular MS lesions. To distinguish a pertiventricular lesion from CSF, the medical expert uses the PD-weighted image, where CSF is not detected. The low-level, single channel segmentation algorithm described here cannot further address the problem of tissue recognition, for example between ventricular CSF and MS lesions. It can be used within an integrated system for MS lesion detection in order to extract convenient topographical and morphological parameters from multispectral MRI data: T1-weighted hypointense and gadolinium-enhanced T1-weighted hyperintense features can be segmented as well as PD and T2-weighted hyperintense features.

To determine whether the binary objects generated by different levels of resolution correspond to complementary or redundant information, it is important to keep track of parameters regarding shape consistency. A 'clearly delimited big' object such as the typical shape of ventricles, corresponds to increasingly bigger binary objects which, at the top of the pyramid, finally gives one binary object (confluent objects). A 'round' object, such as an eye, can be recognized by the consistency of its compactness over different levels of the associated pyramid. A 'consistent contour' can be defined as a list of pixels, which appear in more than one level of resolution as the contour of a binary object. Working out shape parameters such as area, perimeter and compactness would give a morphological signature of an image feature, making its recognition easier.

The sensitivity and the morphological accuracy of the segmentation algorithm is essentially due to the decomposition in the frequency domain of MR images and the local thresholding. The combination of Gaussian decomposition through pyramidal data structures and local thresholding is robust in the presence of radio-frequency inhomogeneity. This must be evaluated in terms of quantitative assessment of MRI lesion load reproducibility, but nevertheless, compared with intensity-based semi-automated segmentation approaches, the proposed technique reduces subjective interventions and improves the overall reproducibility of the quantitative evaluation.

5. Summary

MRI has become the most sensitive paraclinical test to assess the morphology and the topography of MS lesions in the human brain. In order to improve the reproducibility of the quantitative assessment of MS lesions in conventional dual echo spin echo MRI, we propose an automatic segmentation algorithm using a multiresolution approach. Pyramidal data structures are generated for automatic detection of hyperintense features within proton density (PD) and T2-weighted MR images. A given MS lesion is first enhanced at different levels of the corresponding pyramid, depending on its signal intensity and morphology. Then, an automatic and local thresholding algorithm achieves the actual segmentation of the enhanced features. This algorithm does not require any initialization, such as manual or semi-automatic gray-level thresholding or setting initial seeds within a zone of interest. A manual correction, on an acceptance–rejection basis, is needed to remove automatically detected hyperintense features, which are not MS lesions (false positive). The total time needed to process a complete MRI study is much shorter than with manual or semi-automated methods and the reproducibility is improved. The low-level segmentation scheme described in this article may be used for detecting either hyperintense or hypointense features, in the general context of MR image analysis.

Acknowledgements

This work was funded by l'Association pour la Recherche sur la Sclérose En Plaques (ARSEP, 4, rue Chéreau, 75013 Paris, France) and by La Ligue Francaise contre la Sclérose En Plaques (LFSEP, 17 Bd Auguste Blanqui, 75013 Paris, France).

References

[1] Barkhof F. Role of MR imaging in the diagnosis of MS. Adv MRI Contrast 1996;4:31–38.
[2] Confavreux C. Les critères du diagnostic de la sclérose en plaques. Paris: La Presse Médicale (in press).
[3] Grimaud J, Hermier M, Pachai C, Confavreux C. Apport de l'IRM à l'étude de la sclérose en plaques. Revue Neurologique 1997;153:754–770.
[4] Barkhof F. MR imaging in monitoring the treatment of MS: making good use of resources. Adv MRI Contrast 1996;4:46–53.
[5] Barkhof F, Fillipi M, Miller DH, Tofts P, Kappos L, Thompson AJ. Strategies for optimizing MRI techniques aimed at monitoring disease activity in multiple sclerosis treatment trials. J Neurol 1997;244:76–84.
[6] Fillipi M, Horsfield MA, Tofts PS, Barkhof F, Tompson AJ, Miller

DH. Quantitative assessment of MRI lesion load in monitoring the evolution of multiple sclerosis. Brain 1995;118:1602–1612.
[7] Hohol MJ, Guttmann CRG, Orav J, Mackin GA, Kikinis R, Khoury SJ, Jolesz FA, Weiner HL. Serial neuropsychological assessment and magnetic resonance imaging analysis in multiple sclerosis. Arch Neurol 1997;54:1018–1025.
[8] Bedell BJ, Narayana PA, Wolinsky JS. A dual approach for minimizing false lesion classifications on magnetic resonance images. Magn Reson Med 1997;37:94–102.
[9] Zijdenbos A, Evans A, Riahi F, Sled J, Chui J, Kollokian V. Automatic quantification of multiple sclerosis lesion volume using stereotaxic space. Visualization in Biomedical Computing, Proceedings of the 4th International Conference, VBC '96. Hamburg (Germany): Springer, 1996:439–48.
[10] Kamber M, Shinghal R, Collins L, Francis GS, Evans AC. Model-based 3-D segmentation of multiple sclerosis lesions in magnetic resonance brain images. IEEE Trans Med Imaging 1995;14(3):442–453.
[11] Mitchel JR, Karlik SJ, Lee DH, Fenster A. Computer-assisted identification and quantification of multiple sclerosis lesions in MR imaging volumes in the brain. JMRI 1992;4(2):197–208.
[12] Udupa JK, Wei L, Samarasekera S, Miki Y, Van Buchem MA, Grossman RI. Multiple sclerosis lesion quantification using fuzzy-connectedness principles. IEEE Trans Med Imaging 1997;16(5):598–609.
[13] Wells WM, Grimson WEL, Kikinis R, Jolesz FA. Adaptive segmentation of MRI data. IEEE Trans Med Imaging 1996;15(4):429–443.
[14] Narayana PA, Borthakur A. Effect of radio frequency inhomogeneity correction on the reproducibility of intra-cranial volumes using MR image data. Magn Reson Med 1995;33:396–400.
[15] Johnston B, Atkins MS. Segmentation of multiple sclerosis lesions in intensity corrected mutispectral MRI. IEEE Trans Med Imaging 1996;15(2):154–167.
[16] Lippincott, Raven. Magnetic resonance imaging of the brain and spine, 2nd ed. Scott W. Atlas, 1994:653–77.
[17] Bertolino P. Contribution des pyramides irrégulières en segmentation d'images multirésolution. PhD report, Institut National Polytechnique de Grenoble, France, 1995: 166 pp.
[18] Konik H, Laget B, Calonnier M. Segmentation d'images par utilisation de pyramides à base locales. Traitement du Signal 1993;10(4):283–295.
[19] Burt PJ, Adelson EH. The Laplacian pyramid as a compact image code. IEEE Trans Commun 1983;31(4):532–540.
[20] Jolion JM. Analyse d'images: le modèle pyramidal. Traitement du Signal 1990;7(1):5–17.
[21] Chow CK, Kaneko T. Automatic boundary detection of the left ventricle from cineangiograms. Computers and Biomedical Research 1972;5:388–410.
[22] Press WH, Flannery BP, Teukolsky SA, Vetterling WT. Numerical recipes in C—The art of scientific computing, 2nd ed. Cambridge University Press, 1992:123–45.

Chahin Pachai obtained an Electrical and Electronic Engineering degree (1995) and a Master of Science degree in signal and image processing (1996) from the National Institute of Applied Sciences (INSA) of Lyon, France. He is now a Ph.D. student with major focus on various aspects of automatic segmentation of Magnetic Resonance images of human brain.

Yue Min Zhu received a BS degree in Electrical Engineering from Huazon Institute of Technology, Wuhan, China, in 1982. He obtained an MS degree (1984) and a Ph.D.(1988) from INSA of Lyon, France and a Habilitation to conduct research projects in 1993. He is a permanent researcher of the CNRS (The National Center for Scientific Research, France). His current research projects are MR image segmentation, ultrasonic and X-ray image fusion and high resolution X-ray imaging systems. His research interests include time–frequency analysis, multi-resolution analysis, local spectral analysis, image segmentation, data fusion and real-time X-ray imaging.

Jérôme Grimaud, M.D., is a neurologist from the Claude-Bernard University, Lyon, France, working at the Department of Neurology, Hôpital de l'Antiquaille, Lyon, France. He is a member of the European Magnetic Resonance Network in Multiple Sclerosis (MAGNIMS). His research interests include the MRI findings in multiple sclerosis, in terms of sensitivity and specificity.

Marc Hermier, M.D., is a neuroradiologist from the Claude-Bernard University, Lyon, France, working at the neuroradiology and MRI Unit of the Pierre Wertheimer's Neurologic and Neurosurgical Hospital in Lyon, France. His research interests include clinical applications of MRI, especially in multiple sclerosis and pediatric neuroradiology. He is also a Ph.D. student at CREATIS, INSA of Lyon, France, working on medical aspects of automatic segmentation and quantification of cerebral multiple sclerosis lesions in MRI.

Anne Dromigny-Badin, obtained an Engineering degree (1993) from ICPI Lyon, France, a Master of Science degree (1994) in signal and image processing and a Ph.D. degree (1998) on data fusion and image segmentation in industrial and medical contexts from INSA of Lyon, France.

Abdel-Ouahab Boudraa received a University degree in Nuclear Magnetic Resonance in 1993, a Ph.D. degree in Biomedical Engineering in 1994, a University degree in Statistics and Modelisation, in 1995 and a University degree in Positron Emission Tomgraphy in 1997, all from University of Lyon. His current research interests include computer vision, data structures and analysis, hard and fuzzy pattern recognition and applications of fuzzy set theory to mdedical image analysis. Dr. Boudraa is an associate member of IEEE.

Gérard Gimenez, Ph.D., is the Co-director of CREATIS, CNRS Research Unit UMR 5515, Professor at the Department of Electrical Engineering, INSA of Lyon, France and Head of the Ecole Doctorale Electricity, Electrotechnique and Automatism (EEA). His research interests include signal and image processing with particular focus on medical applications.

Christian Confavreux, M.D., Professeur des Universités, Praticien Hospitalier, is the Head of the Department of Neurology, Hôpital de l'Antiquaille, Lyon, France and the Head of NEUROBIOTEC, Institut Fédératif de Recherche des Neurosciences de Lyon, INSERM IFR-19. He is also the Project-leader of the EDMUS (European Database for MUltiple Sclerosis) Coordinating Center and EDMUS Centralized Facility (BIOMED Contracts BMH1-CT93-1529, CIPD-CT94-0227 and BMH4-CT96-0064) and the Vice-President of ECTRIMS (European Committee for Treatment and Research in Multiple Sclerosis).

Jean-Claude Froment, M.D., is Professor of Radiology at the Claude Bernard Lyon-I University, and Head of the Neuroradiology Department of the Pierre Wertheimer Neurologic and Neurosurgical Hospital of Lyon, France. He is a Member of CREATIS, CNRS Research Unit UMR 5515. His main research interests are focused on cerebral MRI and 3D cerebral angiography.